FACTA UNIVERSITATIS
Series: **Electronics and Energetics** Vol. 38, Nº 1, March 2025, pp. 71 - 88
https://doi.org/10.2298/FUEE2501071M

Original scientific paper

THE ESTIMATION OF CHANNEL STATE INFORMATION FOR MULTI-USER LTE SYSTEMS

Subhra Surochita Mishra, Jibendu Sekhar Roy

School of Electronics Engineering, KIIT University, Bhubaneswar, Odisha, India

ORCID iDs: Subhra Surochita Mishra https://orcid.org/0000-0003-1671-385X
Jibendu Sekhar Roy https://orcid.org/0000-0002-3571-2708

Abstract. *The Single carrier frequency division multiple access (SC-FDMA) at the receiver side has a very low power consumption and is considered as the technique for uplink in long-term evolution (LTE). The objective of this paper is to exploit the channel state information (CSI) at the receiver end and then fed back to the transmitter end, until the channel gains in both links are highly correlated or reciprocal. In the uplink channel multiple independent receivers transmit to the eNB in same time-frequency resource. In the downlink channel the eNB transmits data packets to multiple independent user end (UE) in same time-frequency resource. A joint processing is carried out at eNB end called precoding which requires the knowledge of CSI at transmitting end. Exploiting such channel information makes it possible to increase the channel capacity, improve error performance, and at the same time reduce hardware complexity. Here the time division duplexing (TDD) systems are taken because forward and reverse channels tend to be reciprocal. The performance of TDD-based duplex model for multi-user LET-advanced (LTE-A) system is observed for vehicular, pedestrian and typical urban (TU) channel models. In uplink, the obtained bit error rate (BER) at 20 dB signal-to-noise ratio (SNR) for extended pedestrian A (EPA) model is 0.0503 at 5 Hz which is better compared to 0.0664 for extended typical urban (ETU) model at 70 Hz and 0.0625 for extended vehicular A (EVA) model at 70 Hz. But in downlink, the ETU model achieved a BER of 0.0391 at 70 Hz compared to 0.0465 for EVA model at 70 Hz and 0.0451 for EPA model at 5 Hz. The system model performs better for MSE obtained is -19.5640 dB for EPA at 5 Hz in both uplink and downlink.*

Key words: *Channel estimation, LTE, Precoding, channel state information, TDD*

Received July 14, 2024; revised November 21, 2024; accepted November 22, 2024
Corresponding author: Jibendu Sekhar Roy
School of Electronics Engineering, KIIT University, Bhubaneswar, Odisha, India
E-mail: drjsroy@kiit.ac.in

1. Introduction and Related Research Work

The introduction of LTE is aimed at expanding the UTRAN (Universal Terrestrial Radio Access Network). Its development is aimed at achieving the 4G wireless communication. But most importantly, the early objectives [1, 2] for LTE were the required continuity in competition with 3G systems (for higher data rates and superior quality of service (QoS)) in addition to improved packet switching and low latency [3]. Overall, LTE system requirements are based on system capability, System performance with throughput, spectrum efficiency, and mobility. In the LTE E-UTRAN (evolved UMTS terrestrial radio access network) transmission schemes, in the uplink channel multiple independent receivers transmit to the eNB in same time-frequency resource [3]. Overall, the LTE system requires good system capability and performances with enhanced throughput, spectrum efficiency, and mobility [4]. In orthogonal frequency division multiplexing (OFDM), the communication performance can be improved by exploiting the channel information [5]. This channel is referred as MAC (Multiple access channel). The radio access technique in this channel is SC-FDMA, as it shows lower peak-to-average-power ratio (PAPR) value compared with conventional OFDM system. In the downlink channel the eNB transmits data packets to multiple independent UE in same time-frequency resource. This channel is referred as BC (Broadcast channel). The radio access technique in this channel is OFDM [6]. In [7 MoRSE], the performance of SC-FDMA system, under various modulation techniques is reported. In [8], for 5G networks concept of non-orthogonal multiple access (NOMA) to serve more number of users in that same resource block is described. Then different multiplexing techniques in orthogonal multiple access with modulation schemes are studied in [9]. The improved performances of SC-FDMA, using different sub-carrier mapping methods are presented in [10 ASEAN]. For wireless system, one promising technique intelligent reflecting surfaces (IRSs) is used to increase the energy efficiency [11]. Different models of path loss (PL) for performance and network coverage estimation are required for optimization in IOT technology [12]. The performance of SC-FDMA under heavily faded areas is reported in [13 AEEE]. In the TDD/FDD (frequency division duplexing) systems within the 6 GHz band under the indoor corridor, to extract the components of multipath an algorithm is proposed for the channel reciprocity [14]. Wireless channels characterization can be done by two aspects that are channel reciprocity and PL [15]. In the uplink the transmitters are hand-held mobile terminals driven by battery. The performance of the transmitter reduces with OFDM as the access technology due to its high PAPR. The LTE standard introduces a DFT spread orthogonal frequency division multiple accessing (OFDMA) called SC-FDMA as the access technology for uplink due to its lower PAPR value. In an effort to reduce the power consumption of the terminal, the LTE Uplink uses SC-FDMA, because uplink transmission needs a PAPR that is low considering the need for higher bit rates. As the receivers (UE) are autonomous units joint processing for interference cancellation cannot be carried out at receiving end. Hence, the joint processing is carried out at eNB end called Precoding. The precoding process requires the knowledge of CSI at transmitting end. In OFDMA, the spectrum is essentially divided into a series of uniform orthogonal narrowband subcarriers; with each subcarrier at 15 kHz spacing and corresponding modulation symbols. For the duration of 1 symbol, the number of subcarriers is orthogonally transmitted in the frequency domain. To avoid inter carrier interference (ICI) and for efficient use of the spectrum, one sub-carrier spectrum's peak must coincide with the other sub-carrier's zeros, hence creating zero ICI. A common approach in OFDM systems like LTE and 5G is to perform channel estimation in the frequency domain. Several studies have focused on

frequency-domain methods, which leverage the sparsity of the channel in the frequency domain to achieve efficient and accurate estimation. This method reduces the complexity compared to time-domain estimations, especially in systems with frequency-selective fading. The paper [16] provides an overview of the emerging technologies in 5G, including advances in channel estimation techniques. The work in [17] discusses frequency-domain techniques for channel estimation in MU-MIMO systems, a key technology for 5G. In contrast to frequency-domain techniques, time-domain estimation often involves using pilots or training sequences to estimate the channel impulse response. Though more computationally intensive, time-domain methods can offer higher accuracy in non-frequency selective channels. This study [18] compares time-domain estimation techniques with frequency-domain methods, highlighting their strengths in certain network conditions. Precoding is essential for improving the performance of multi-user MIMO systems by reducing inter-user interference and maximizing the signal-to-interference-plus-noise ratio (SINR). Various precoding strategies have been proposed to optimize transmission in systems like LTE and 5G. Linear precoding techniques, such as Zero-Forcing (ZF) and Maximum Ratio Transmission (MRT), are widely used because of their simplicity and effectiveness in certain interference environments. These methods typically operate in the frequency domain, allowing them to align with the characteristics of OFDM systems. The paper [19] discusses different precoding schemes for multi-user MIMO systems and their application in systems like LTE and 5G. The work [20] explores the use of linear precoding in large antenna arrays, relevant for next-generation mobile networks. Techniques such as Tomlinson-Harashima Precoding (THP) and Block Diagonalization (BD) offer potential performance improvements over linear methods but at the cost of higher computational complexity. The paper [21] discusses non-linear precoding strategies and their impact on system performance. Hybrid techniques that combine time-domain and frequency-domain methods for both channel estimation and precoding have emerged to capitalize on the strengths of both approaches. These methods are particularly useful in scenarios involving dynamic channels and mixed traffic types, where a hybrid approach can adapt to varying network conditions. The paper [22] explores hybrid channel estimation and precoding strategies to improve system performance. The work in [23] surveys the hybrid precoding techniques for 5G systems, focusing on the combination of time and frequency-domain methods.

LTE networks continue to be the backbone of mobile communication systems worldwide. Many regions, especially in developing countries, rely heavily on LTE due to delayed 5G deployments or cost barriers to upgrading infrastructure. 5G networks often coexist with LTE, particularly in the early phases of 5G adoption. Numerous devices and applications still rely on LTE technology, including Internet of Things (IoT) systems, vehicular networks, and rural broadband services. LTE systems use foundational technologies such as SC-FDMA, OFDMA, MIMO, and advanced modulation schemes, which are also integral to 5G [24]. In the initial stages of 5G adoption, many networks are deployed in a Non-Standalone (NSA) configuration, where LTE provides the control plane (signaling and network management), and 5G NR (New Radio) handles the user plane (high-speed data transfer). In areas where 5G coverage is limited or unavailable, LTE serves as a fallback network to ensure uninterrupted connectivity [25]. LTE variants like LTE-M and NB-IoT are optimized for IoT use cases, offering low-power, wide-area connectivity that complements 5G capabilities. These technologies support applications like smart metering, industrial automation, and smart agriculture, which coexist with high-speed 5G use cases. While 5G supports data-driven services, Voice over LTE (VoLTE) remains the dominant standard for high-quality voice

communication. LTE continues to provide voice services for 5G users through integration with IP Multimedia Subsystem (IMS) [24, 26].

In this paper, the channel reciprocity at the receiving end is exploited by knowing the CSI. The estimation of CSI is done in uplink using pilot signals in the slot allocated for this purpose which is utilized by eNB for post equalization for uplink and per-coding for downlink. We further provide analysis of presented method for a TDD-based duplex model for multi-user LTE-A system. The paper is organized as follows: Section 2 describes the system briefly used for simulation. In Section 3, the proposed system model used for the estimation of CSI and its mathematical background are outlined. The simulated results for mean square error (MSE) and bit error rate (BER) for different multi-user systems are presented in Section 4. The conclusion is presented in section 5.

2. SYSTEM DESCRIPTION

Sometimes only statistical channel state information may be available and it makes possible to increase channel capacity, to improve error performance, and to reduce hardware complexity. In [27] a method for channel prediction conditional generative adversarial network (CPcGAN) for TDD/FDD systems is proposed. Also in mmWave channels correct CSI is obtained with less hardware complexity and overhead of pilot signals [28]. The IRS in a TDD-MIMO (multiple input multiple output) system is investigated in [29] where a deep reinforcement learning (DRL) scheme is used to maximize the average downlink data transmission. But practically, the full CSI is unavailable because of the feedback overhead and delay. The transmitter cannot observe the CSI for a time-varying channel completely and so only statistical information can be used. The transmitter generally doesn't have direct access to its own CSI and the access is done indirectly. In a TDD system, channel reciprocity between opposite links (downlink and uplink) can be used. Using the received signal from the opposite side, indirect estimation of channel is possible. The state of the channel in one direction (Fig. 1) can be implicitly known from the other direction. There is an appreciable difference between their transfer times. However, if the difference relative to the coherence time is small, reciprocity can be a useful property to exploit. In general, the RF characteristics of forward channels and the reverse channels are different and by using channel reciprocity this difference can be compensated.

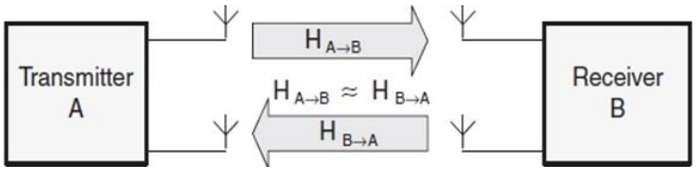

Fig. 1 Reciprocity of wireless channel

The channel state at the transmitter side can be obtained from the receiver feedback, as shown in Fig. 2. Unlike using reciprocity, this method does not require compensation for the RF difference. However, for timely channel information, the feedback delay Δ_t should be less than the coherence time T_c, that is [30]

$$\Delta_t = T_C \tag{1}$$

Its main disadvantage is that an additional source is required to transmit feedback information. The more number of antennas are required for more feedback information. Therefore, for a system with multiple antennas, the overhead delay is a critical issue. An experimental study of channel reciprocity to measure the CSI in both TDD and FDD modes is presented in [31].

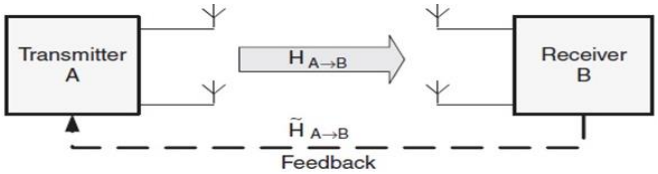

Fig. 2 Feedback process of CSI

3. System Model for the Estimation of Channel State Information

The time division duplex model in multi-user system includes both MAC and BC with access technologies SC-FDMA and OFDM respectively; both are separated in time. Consider a multi-user system with number of UE served by eNB per time-frequency grid is *N*; eNB is equipped with same number of antenna elements. The block diagram of the eNB for the TDD-based system is shown in Figure 3. In the TDD-based frame structure the estimation slot repeats every 0.5 ms, where, six symbols for payload data; alternatively used by both references. In LTE and similar systems, the sub-frame duration is 1 ms, divided into two slots of 0.5 ms each. This ensures synchronization between uplink (UL) and downlink (DL) transmissions in time division duplex (TDD) mode. A 0.5 ms duration balances the overhead for estimation slots and the slots reserved for payload data transmission. Shorter duration, such as 0.25 ms, may lead to increased switching times and processing complexity, while longer durations (e.g., 1 ms) might result in inefficiencies for real-time applications and would increase overhead. The model is designed for asynchronous data transfer, most suitable for Internet traffic. The number of symbols carried per sub-carrier in each symbol is one for uplink, as the SC-FDMA symbol of each user maintains frequency domain orthogonality among each other whereas for downlink the number of symbols carried per sub-carrier in each symbol is *N*.

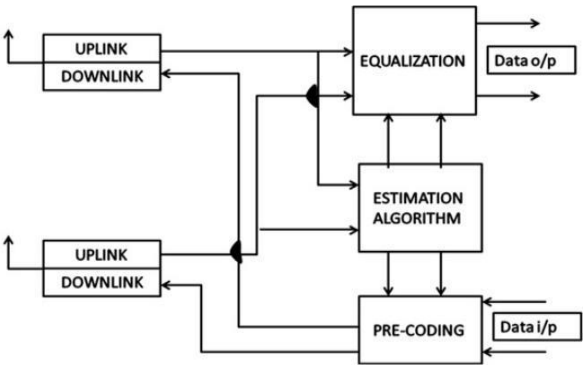

Fig. 3 Functional System Model of eNB for TDD system

3.1. Uplink Phase

The symbol next to the estimation symbol is used for uplink and then every alternative symbols are used for same purpose. In this phase N numbers of UE transmit SC-FDMA data packets to eNB in same time-frequency resource; each data bit is spreaded over $U = M/N$ sub-carriers and mapped in M sub-carriers using a distributive mapping function. Considering *n-th* slot is for the uplink ($1 < n < 7$), let $x_i^n(p)$ is the *p-th* element of input modulated data of *i-th* UE in *n-th* SC-FDMA symbol, undergoes N-point DFT spreading, mapped into M sub-carriers providing the frequency domain signal of *i-th* UE [32]

$$S_i^n[k] = D_i\left[\frac{1}{\sqrt{N}}\sum_{p=0}^{N-1} x_i^n(p)\exp\left(\frac{-j2\pi pk}{N}\right)\right] \tag{2}$$

where $D_{(i)}[.]$ is the mapping function for *i-th* UE and k is the sub-carrier index. The frequency domain signal undergoes M point IFFT before transmission and the corresponding signal at sample time m is given by

$$S_i^n[m] = \left[\sum_{k=0}^{M-1} S_i^n[k]\exp\left(\frac{-j2\pi mk}{M}\right)\right] \tag{3}$$

The received signal at *j-th* antenna of eNB is

$$y_j^n[m] = \sum_{i=1}^{N} h_{i,j}^n * S_i^n(m) + w(m) \tag{4}$$

where $h_{i,j}^n$, is the temporal impulse response of channel between *i-th* UE and *j-th* antenna of eNB during *n-th* symbol. After the cyclic prefix is removed, the FFT output at *k-th* sub-carrier is given as

$$Y_j^n[k] = \sum_{i=1}^{N} H_{i,j}^n \cdot S_i^n(k) + W(k) \tag{5}$$

Here, $H^n_{i,j}[k]$ is the gain associated with the *k-th* subcarrier of the channel between *i-th* UE and *j-th* antenna of eNB during *n-th* symbol and $W(k)$ is the frequency domain representation of additive noise. Due to orthogonality maintained by mapping functions, the signal received for *k-th* sub-carrier is the response of any one of N users.

The estimate of frequency domain signal vector is determined with zero-forcing (ZF) detection technique [33]

$$\hat{S}^{n,k} = \{H^{n,k}\}\cdot Y^{n,k} = \{\hat{H}^k\}^{-1}\cdot Y^{n,k} \tag{6}$$

where, $Y^{n,k} = [Y_1^n[k]\cdots Y_j^n[k]\cdots Y_N^n[k]]^H$ and $\{H^{n,k}\}$ is the channel matrix in frequency domain during *n-th* slot associated with *k-th* sub-carrier.

3.2. Downlink Phase

Considering *n-th* symbol for uplink, the $(n+1)$-*th* symbol is used for downlink where eNB transmits independent data stream to N UE in same time-frequency grid. Unlike uplink, the access technology for downlink is OFDM; as each downlink stream uses all the available sub-carriers, a virtual spatial multiplexing method is established and the number

of simultaneous bits transmitted per time-frequency resource is *N*. Here interference cancellation is the major issue; as the receiver units are autonomous, pre-cancellation of interference has to be carried out at eNB. To achieve optimal spectrum utilization, the reciprocity between both links is exploited providing the channel matrix for downlink for *k-th* sub-carrier as [34]

$$\{\mathrm{C}^{n+1,k}\} \cong \{H^{n,k}\}^{H} \tag{7}$$

Let $E^{n+1}[k]$ is the transmit vector in downlink for *k-th* subcarrier in *(n+1)-th* symbol where its *i-th* element is the data symbol in frequency domain for *k-th* sub-carrier of *i-th* UE. The signal vector that is precoded for *k-th* sub-carrier is given as

$$P^{n+1}[k] = \{\mathrm{C}^{n+1,k}\} \cdot E^{n+1}[k] \tag{8}$$

For $P_j^{n+1}[k]$ be the *j-th* element of $P^{n+1}[k]$, the time domain signal transmitted from *j-th* antenna of eNB is given as

$$C_j^{n+1}[m] = \sum_{k=0}^{M-1} P_j^{n+1}[k] exp\left(\frac{j2\pi mk}{M}\right) \tag{9}$$

The precoding scheme in equation (8) is chosen because it optimizes the system's performance in terms of interference mitigation, adaptability to dynamic channel conditions, and computational efficiency. It ensures scalable, fair, and efficient transmission for multiple users in modern communication systems like LTE and 5G. By leveraging channel state information and linear precoding, it provides an effective solution for high-capacity, low-latency, multi-user environments.

Compared to more complex schemes such as nonlinear precoding (e.g., Tomlinson-Harashima Precoding) or block diagonalization, the linear precoding method in equation (8) offers a good balance between computational complexity and performance [35, 36]. While these more complex methods can offer better interference cancellation, the linear precoding used here is computationally simpler and efficient, making it suitable for real-time applications where low-latency performance is required.

3.3. Estimation Phase

The estimation quality is important for system performance; the major concern of the estimation process for MU-MIMO system [37] is with the limited spectrum overhead and computational complexity, it has to cope up with issues like transmit diversity and tracking of time-varying channel parameters involved in each path. This challenge of MU-MIMO estimation process can be overcome by using advanced signal processing technique [38]. In TDD based model estimation is done in uplink and is utilized for both links assuming the reciprocity between them.

The estimation of the channel is done by putting reference (pilot) signal in MAC during the slot allocated for that. The frequency domain received signal at *j-th* antenna of eNB in *k-th* sub-carrier is [39]

$$Y_j[k] = \sum_{i=1}^{N} H_{i,j}[k] \cdot R_i[k] + W[k] \tag{10}$$

Where $H_{i,j}$[k] is the channel gain between *i-th* UE and *j-th* antenna of eNB, R_i[k] is the signal transmitted from *i-th* UE and *W*[k] is the noise associated with the path in *k-th* sub-carrier. In the estimation slot each UE transmits independent reference signal strings interleaved with null sub-carriers; frequency domain orthogonality is maintained among each other to combat transmit diversity problem. The *i-th* UE puts its reference bits in the *k-th* sub-carrier which is given by

$$k = (i + p \times N) \tag{11}$$

where *M* is the number of sub-carriers present, i =1,2,…,*N* and p = 0,1,2,… referring reference bit bearing sub-carrier index and rest are null sub-carriers. As each sub-carrier is associated with one UE, considering *k* as the reference bit bearing sub-carrier index of i-th UE, the equation (10) reduces to

$$Y_j[k] = H_{i,j}[k] \cdot R_i[k] + W[k] \tag{12}$$

The least-square (LS) estimate of channel gain is given as

$$\hat{H}_{i,j}[k] = \frac{Y_j[k]}{R_i[k]} \tag{13}$$

The LS estimator presented in this work is applied in the frequency domain, which aligns with the OFDM modulation used in modern systems like LTE and 5G. This approach leverages the structure of the frequency-domain transmission, where each subcarrier is independently estimated, allowing for efficient computation and effective handling of frequency-selective fading. While time-domain channel estimation, as discussed in [40], is a valid approach, it introduces additional complexity in terms of symbol interference and computational cost, especially in systems with large bandwidths. The frequency-domain approach provides a simpler, computationally efficient alternative that is more suited to the multi-carrier nature of the system.

The estimation of complete channel transfer function (CTF) is done interpolating the information obtained in equation (5); DFT-based smoothing technique is employed to remove effect of noise outside the maximum channel delay [41]. The channel matrix for *k-th* sub-carrier is $\{\hat{H}^k\}$ where each (*i;j*)*-th* entry is given by $\hat{H}^n_{i,j}[k]$. This estimate is utilized in intermediate payload symbols assuming

$$\{H^{n,k}\} = \{\hat{H}^k\} \tag{14}$$

4. Results and Discussions for Multi-user Systems

In this section the performance of TDD based duplex model for multi-user LTE-A system is observed in the simulation. The channel considered are Extended Typical Urban model (ETU), Extended Vehicular A model (EVA) and Extended Pedestrian A model (EPA). Based on some physical factors in the urban dense street scenarios channel modelling is done for MIMO systems [42]. The estimation of CSI is done in uplink using pilot signals in the slot allocated for this purpose which is utilized by eNB for post equalization for uplink and per-coding for downlink. The simulation parameters are shown in Table 1.

Table 1 Simulation specifications

System Parameters		
Specifications:	No. of UE	02
	No. of antenna in eNB	02
	Modulation type	QPSK
In Uplink:	Air interface	SC-FDMA
	Size of FFT	512
	Mapping scheme	Distributive
In Downlink:	Air Interface	OFDM
	Size of FFT	512
	Cyclic prefix length	10
Channel Specifications:	Channel type	ETU, EVA, EPA
	Max. Doppler shift	5 Hz, 70 Hz ,300 Hz
	r.m.s delay spread	0.356 μs

The Fig. 4 and Fig. 5 show the MSE in process of estimation and uncoded BER performances respectively of the presented duplex model with maximum Doppler shift of 70 Hz and 300 Hz.

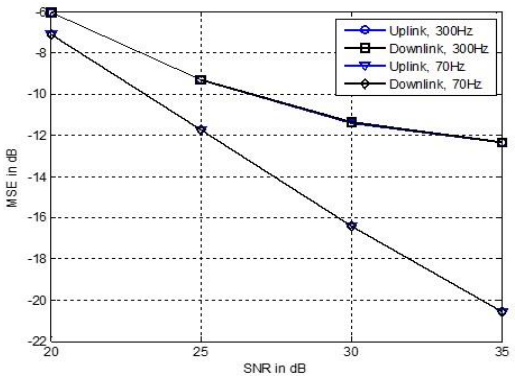

Fig. 4 MSE performance with maximum Doppler shift of 70 Hz and 300 Hz

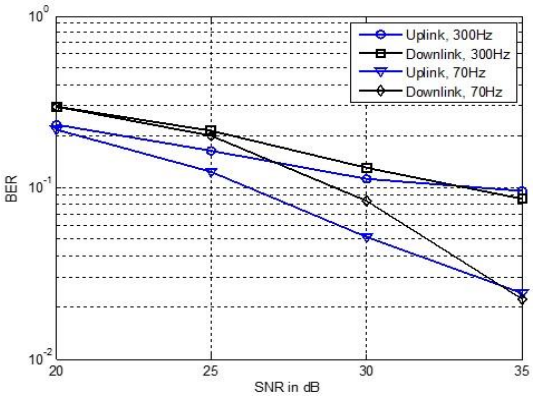

Fig. 5 Performance of BER with maximum Doppler shift of 70 Hz and 300 Hz

The delay profiles for the multi-path propagation models in ETU, EVA, and EPA are given in Table 2. Doppler shifts are integrated to obtain the Doppler power spectral density (PSD) in each path [43].

Table 2 Delay profiles for ETU, EVA, and EPA

Channel	Maximum Doppler Frequency	Excess Tap Delay	Delay Profile
ETU	70 Hz, 300 Hz	[0 50 120 200 230 500 1600 2300 5000]	[-0.1 -0.1 -0.1 0.0 0.0 0.0 -3.0 -5.0 -7.0]
EVA	5 Hz, 70 Hz	[0 30 150 310 710 1090 1730 2510]	[0.0 -1.5 -1.4 -3.6 -9.1 -7.0 -12.0 -16.9]
EPA	5 Hz	[0 30 70 90 110 190 410]	[0.0 -1.0 -2.0 -3.0 -8.0 -17.2 -20.8]

The Fig. 6 and Fig. 7 show the uncoded BER and MSE performances in process of estimation respectively of the presented duplex model by varying the number of pilots spacing for extended typical urban (ETU) model at 70 Hz Doppler frequency.

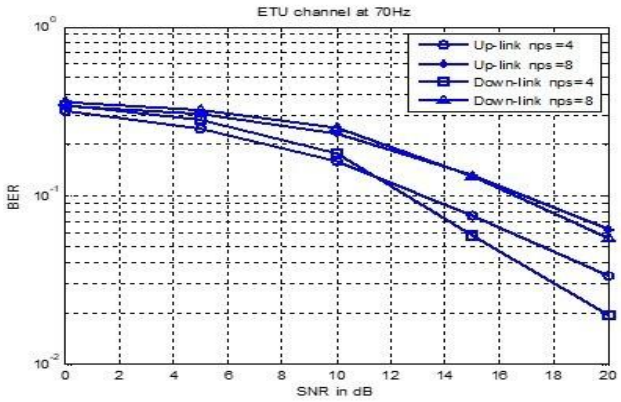

Fig. 6 Performance of BER of ETU model at 70 Hz

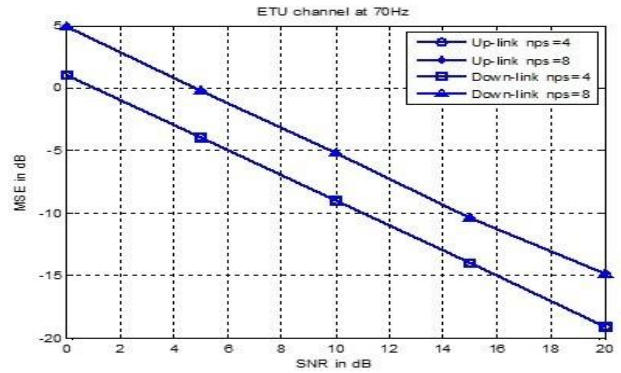

Fig. 7 MSE performance of ETU model at 70 Hz

The Fig. 8 and Fig. 9 show the uncoded BER and MSE performances in process of estimation respectively of the presented duplex model by varying the number of pilots spacing for extended typical urban (ETU) model at 300 Hz Doppler frequency.

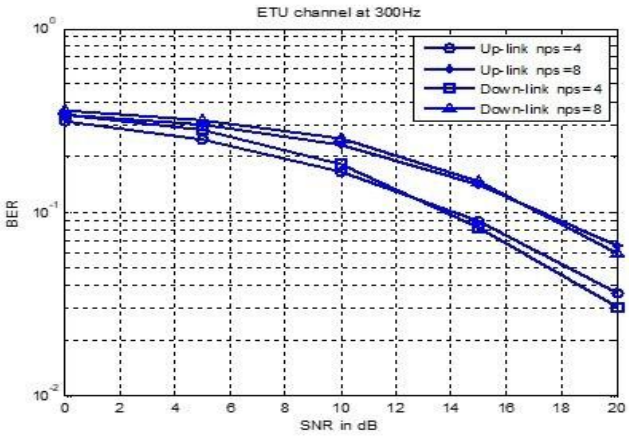

Fig. 8 Performance of BER of ETU model at 300 Hz

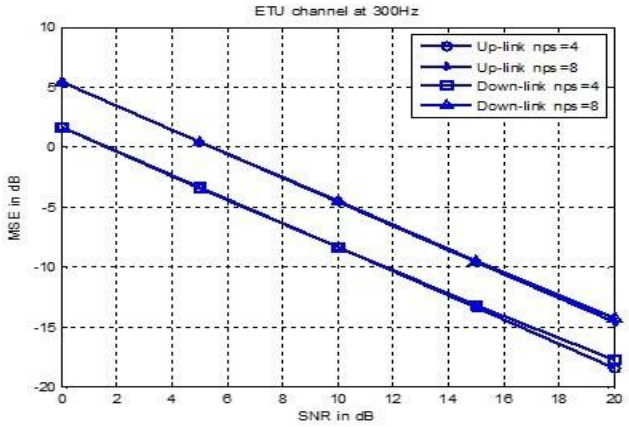

Fig. 9 MSE performance of ETU model at 300 Hz

The Fig. 10 and Fig. 11 show the uncoded BER and MSE performances in process of estimation respectively of the presented duplex model by varying the number of pilots spacing for extended vehicular A (EVA) model at 5 Hz Doppler frequency.

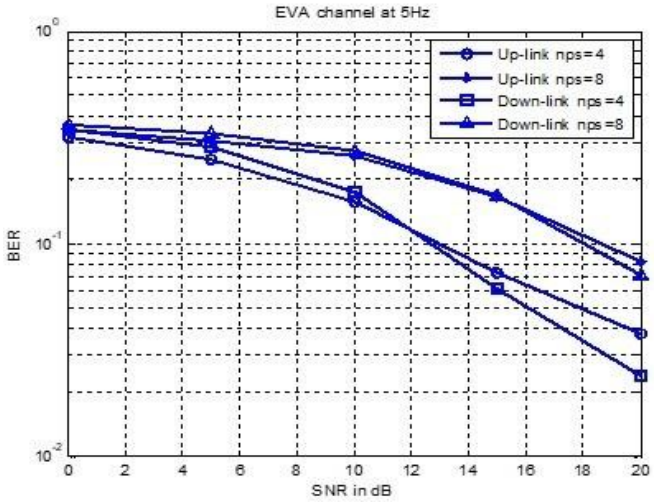

Fig. 10 Performance of BER of EVA model at 5 Hz

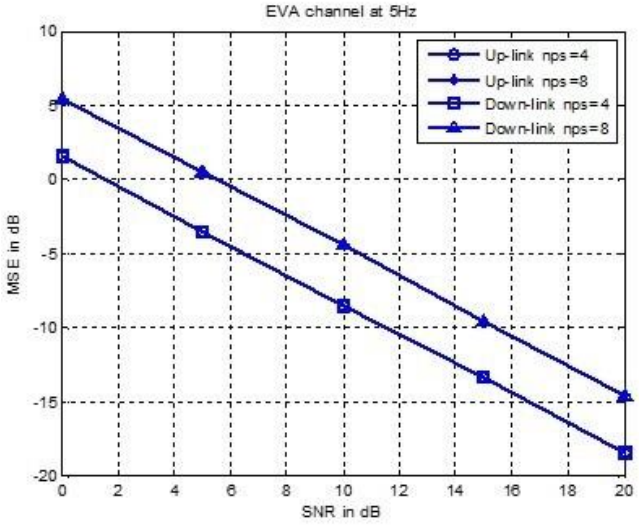

Fig. 11 MSE performance of EVA model at 5 Hz

The Fig. 12 and Fig. 13 show the uncoded BER and MSE performances in process of estimation respectively of the presented duplex model by varying the number of pilots spacing for extended vehicular A (EVA) model at 70 Hz Doppler frequency.

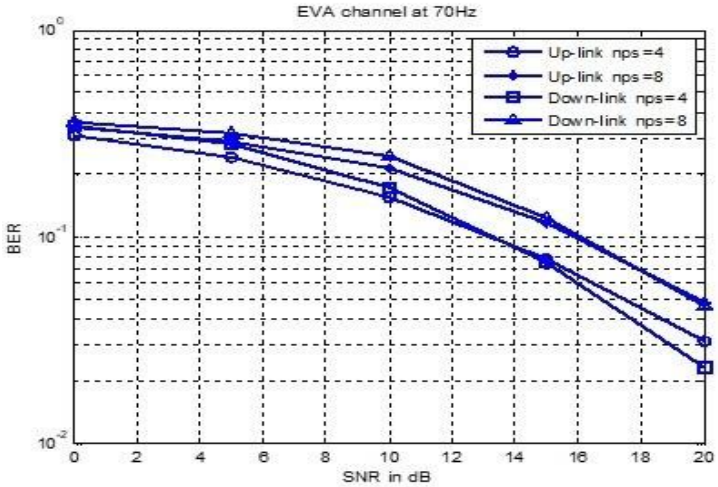

Fig. 12 Performance of BER of EVA model at 70 Hz

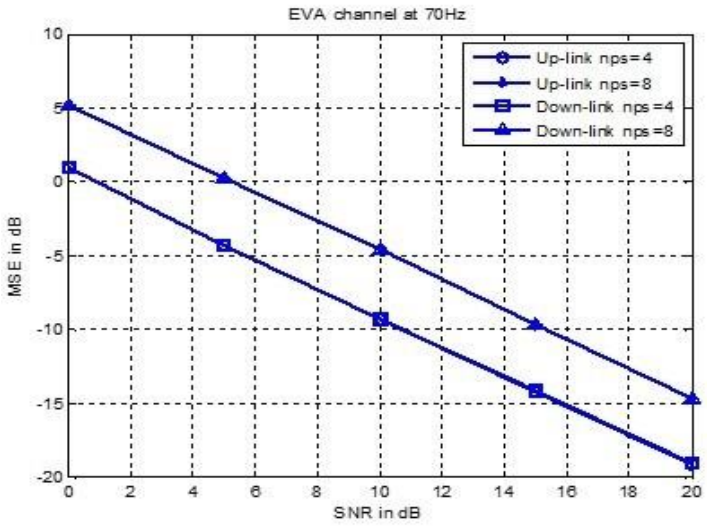

Fig. 13 MSE performance of EVA model at 70 Hz

The Fig. 14 and Fig. 15 show the uncoded BER and MSE performances in process of estimation respectively of the presented duplex model by varying the number of pilots spacing for extended pedestrian A (EPA) model at 5 Hz Doppler frequency.

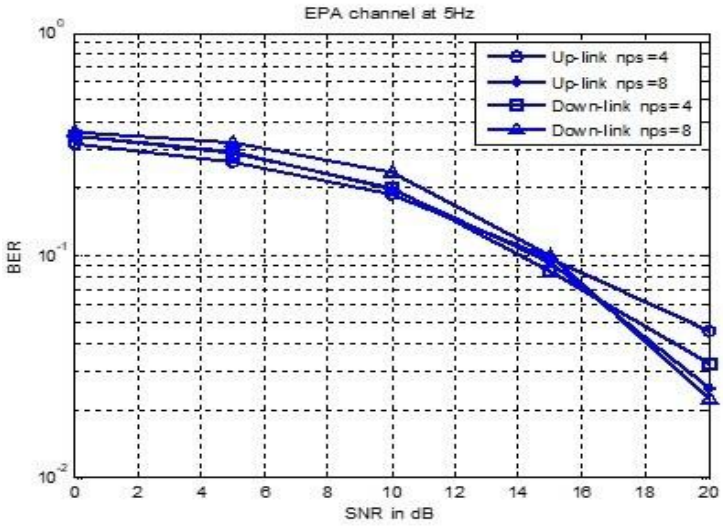

Fig. 14 Performance of BER of EPA model at 5 Hz

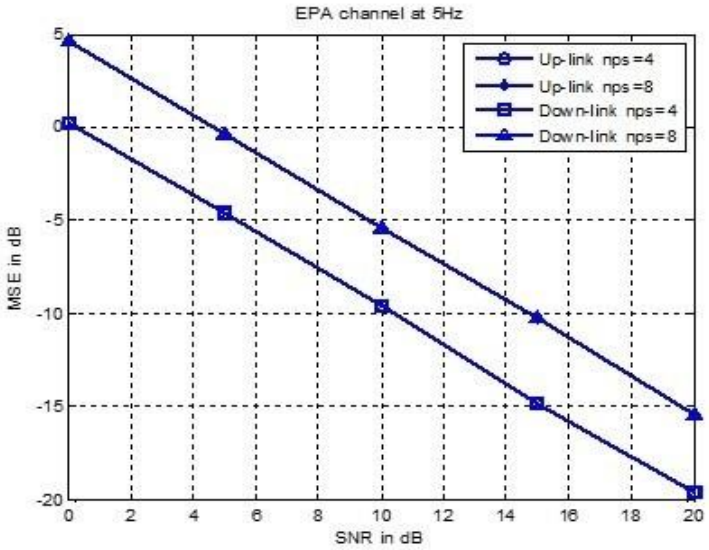

Fig. 15 MSE performance of EPA model at 5 Hz

The performances of multi-user systems in relation to estimation of CSI are tabulated in Table 3.

Table 3 Comparison between ETU, EVA and EPA channel models

Channel	Maximum Doppler Frequency	Pilot Spacing	SNR (dB)	Uplink		Downlink	
				BER	MSE (dB)	BER	MSE (dB)
ETU	70 Hz	4	0	0.6288	1.0458	0.6895	1.0472
			10	0.3188	-9.0211	0.3548	-9.0147
			20	0.0664	-19.1216	0.0391	-19.0731
	70 Hz	8	0	0.6808	4.8732	0.7113	4.8731
			10	0.4641	-5.1731	0.5046	-5.1708
			20	0.1264	-14.8745	0.1109	-14.8732
	300 Hz	4	0	0.6260	1.6522	0.6793	1.6660
			10	0.3329	-8.4119	0.3664	-8.3492
			20	0.0724	-18.4800	0.0611	-17.7591
	300 Hz	8	0	0.6796	5.3510	0.7126	5.3579
			10	0.4616	-4.5626	0.5019	-4.5328
			20	0.1311	-14.5930	0.1184	-14.2921
EVA	5 Hz	4	0	0.6336	1.4929	0.6902	1.4929
			10	0.3126	-8.5342	0.3512	-8.5341
			20	0.0749	-18.4986	0.0478	-18.4987
	5 Hz	8	0	0.6878	5.3847	0.7191	5.3848
			10	0.5193	-4.4590	0.5431	-4.4593
			20	0.1647	-14.5855	0.1423	-14.5857
	70 Hz	4	0	0.6184	0.9230	0.6847	0.9231
			10	0.3087	-9.3541	0.3451	-9.3549
			20	0.0625	-19.1495	0.0465	-19.1014
	70 Hz	8	0	0.6757	5.1026	0.7144	5.1012
			10	0.4309	-4.6363	0.4883	-4.6350
			20	0.0956	-14.7204	0.0924	-14.7214
EPA	5 Hz	4	0	0.6348	0.2461	0.6857	0.2461
			10	0.3718	-9.5800	0.4025	-9.5797
			20	0.0913	-19.5640	0.0647	-19.5639
	5 Hz	8	0	0.6828	4.5635	0.7128	4.5634
			10	0.3953	-5.4160	0.4674	-5.4161
			20	0.0503	-15.4320	0.0451	-15.4323

In Table 2, in ETU model, the maximum Doppler frequency is considered to be 70 Hz and 300 Hz for 4 and 8 number of users. Similarly for EVA model, the maximum Doppler frequency is considered to be 5 Hz and 70 Hz for 4 and 8 number of users and for EPA model the maximum Doppler frequency is considered to be 5 Hz for 4 and 8 number of users. The simulation results shows that in uplink, the BER at 20 dB SNR for EPA model is 0.0503 at 5 Hz which is better compared to 0.0664 for ETU model at 70 Hz and 0.0625 for EVA model at 70 Hz. But in downlink, the ETU model achieved a BER of 0.0391 at 70 Hz compared to 0.0465 for EVA model at 70 Hz and 0.0451 for EPA model at 5 Hz. The system model performs better for MSE obtained is -19.5640 dB for EPA at 5 Hz in both uplink and downlink. The system model performs better for MSE obtained is -19.5640 dB for EPA at 5 Hz in both uplink and downlink.

5. CONCLUSION

In this paper, we have studied the SC-FDMA, which is considered the technique for uplink in LTE, and the process of precoding, which requires knowledge of the CSI at the transmitting end. On the transmission end, CSI may be fully or partially known. With the proposed method, exploiting such channel information makes it possible to increase channel capacity, improve error performance, and at the same time reduce hardware complexity. Based on the obtained results, the performance of a TDD-based duplex model for a multi-user LTE-A system is investigated. The estimation of CSI is done in uplink using pilot signals in the slot allocated for this purpose, which is utilized by eNB for post equalization for uplink and per-coding for downlink. Therefore, the CSI should be estimated at the receiver end and then fed back to the transmitter end.

REFERENCES

[1] S. Sesia, I. Toufik and M. Baker (Edited), *LTE - The UMTS Long Term Evolution, from Theory to Practice,* 2nd Ed., Wiley Publishers, 2011.

[2] P. Humblet and A. Richardson, "Femtocell Radio Technology", *Airvana Corporation Whitepaper*, May 2010.

[3] UTRA-UTRAN Long Term Evolution (LTE) and 3GPP System Architecture Evolution (SAE) Long Term Evolution of the 3GPP Radio Technology, Technical Papers, 2008.

[4] Y. S. Cho, J. Kim, W.Y. Yang and C.G. Kang, *MIMO-OFDM Wireless Communications with MATLAB,* John Wiley & Sons (Asia) Pte Ltd, 2010.

[5] A. Petroni, G. Scarano, R. Cusani and M. Biagi, "On the Impact of Channel State Information Quantization and Feedback in Practical OFDM Implementation", *IEEE Commun. Lett.*, vol. 28, no. 2, pp. 278-282, Feb. 2024.

[6] K. H. Chung, "On Negative Correlation Bit-to-symbol(B2S) Mapping for NOMA with Correlated Information Sources in 5G Systems", *J. KIECS*, vol. 15, no. 5, pp. 881-888, 2020.

[7] J. S. Roy and S. S. Mishra, "Performance of SC-FDMA for LTE Uplink Under Different Modulation Schemes", In Proceedings of the IEEE International Conference on Mechatronics, Robotics and Systems Engineering (MoRSE), Bali, Indonesia, 2019, pp. 202-206.

[8] M. Vaezi, R. Schober, Z. Ding and H. V. Poor, "Non-orthogonal Multiple Access: Common Myths and Critical Questions", *IEEE Wireless Commun.*, vol. 26, no. 5, pp. 174-180, Oct. 2019.

[9] Y. Cai, Z. Qin, F. Cui, G. Y. Li and J. A. McCann, "Modulation and Multiple Access for 5G Networks", *IEEE Commun. Surveys Tuts*., vol. 20, no. 1, pp. 629-646, 2018.

[10] S. S. Mishra and J. S. Roy, "Comparison of Performances Between SC-FDMA and OFDMA Systems Under Different Sub-carrier Mapping Schemes"," *ASEAN Eng. J.*, vol. 13, no. 2, pp. 19-23, May, 2023.

[11] C. Pan, H. Ren, K. Wang, J. F. Kolb, M. Elkashlan, M. Chen, M. Di Renzo, Y. Hao, J. Wang, A. L. Swindlehurst, X. You and L. Hanzo, "Reconfigurable Intelligent Surfaces for 6G Systems: Principles, Applications, and Research Directions", *IEEE Comm. Mag.*, vol. 59, no. 6, pp. 14-20, Jun. 2021.

[12] I. Batalha, A. Lopes, W. Lima, Y. Barbosa, M. Neto, F. Barros and G. Cavalcante, "Large-scale Modeling and Analysis of Uplink and Downlink Channels for LORA Technology in Suburban Environments", *IEEE Internet Things J.*, vol. 9, no. 23, pp. 24477-24491, Dec. 2022.

[13] S. S. Mishra and J. S. Roy, "SC-FDMA Uplink System in Heavily Faded Areas with Low Signal-to-Noise Ratio", *Adv. Electr. Electron. Eng.*, vol. 21, no. 3, pp. 206-215, June 2023.

[14] H. Xu, J. Zhang, P. Tang, L. Tian, Q. Wang and G. Liu, "An Empirical Study on Channel Reciprocity in TDD and FDD Systems", *IEEE Open J. Veh. Technol.*, vol. 5, pp. 108-124, 2024.

[15] W. Tang, J. Wang, J. Y. Dai, M. Di Renzo, S. Jin, Q. Cheng and T. J. Cui, "On Path Loss and Channel Reciprocity of RIS-assisted Wireless Communications", in *Intelligent Surfaces Empowered 6G Wireless Network*, Wiley, pp.37-58, 2024.

[16] A. Gupta and R. K. Jha, "A Survey of 5G Network: Architecture and Emerging Technologies", *IEEE Access*, vol. 3, pp. 1206-1232, 2014.

[17] H. Zhang et al. "Frequency-domain Channel Estimation for Multi-user MIMO Systems," *IEEE Trans. Wirel. Commun.*, vol. 15, no. 10, pp. 7023-7034, 2016.

[18] Y. Yu and W. Wu, "Channel Estimation for MIMO-OFDM Systems in Time Domain", *IEEE Trans. Wirel. Commun.*, vol. 3, no. 3, pp. 809-818, 2004.
[19] D. Gesbert, M. Kountouris, R. W. Heath, C. -B. Chae and T. Salzer, "From Single-user to Multi-user Communications: Shifting the Paradigm", *IEEE Trans. Wirel. Commun.*, vol. 7, no. 6, pp. 2093-2103, 2007.
[20] J. Hoydis, S. ten Brink and M. Debbah, "Massive MIMO: How Many Antennas do We Need?", In Proceedings of the 49th Annual Allerton Conference on Communication, Control, and Computing (Allerton), Monticello, IL, USA, 2011, pp. 545-550.
[21] H. Li and J. Liu, "Nonlinear Precoding for Multi-user MIMO Systems," *IEEE Trans. Signal Process*., vol. 60, no. 6, pp. 2992-3002, 2012.
[22] J. Kim et al., "Hybrid Channel Estimation and Precoding for Multi-user Massive MIMO Systems", *IEEE Trans. Wirel. Commun.*, vol. 15, no. 4, pp. 2672-2684, 2016.
[23] D. Lee et al., "Hybrid Precoding for 5G: A survey", *IEEE Access*, vol. 8, pp. 88712-88729, 2020.
[24] M. Deepender, U. Shrivastava and J. K. Verma, "A Study on 5G Technology and Its Applications in Telecommunications", In Proceedings of the International Conference on Computational Performance Evaluation (ComPE), Shillong, India, 2021, pp. 365-371.
[25] R. Kumar, I. Singh, A. Alkhayyat, A. Joshi, A. Badhoutiya and S. Singh, "5G: Radio Technology Crafted for Wireless Cellular Connectivity", In Proceedings of the 11th International Conference on Computing for Sustainable Global Development (INDIACom), 2024, pp.721-726.
[26] Lovekesh, M. Yadav and D. Nandal, "Exploring 5G Architecture, Technologies, and Mobility Challenges: A Path to SDN-Based Future", In Proceedings of the International Conference on Advanced Computing & Communication Technologies (ICACCTech), 2023, pp. 551-558.
[27] Z. Zhang, Y. Zhang, J. Zhang and F. Gao, "Adversarial Training-aided Time-varying Channel Prediction for TDD/FDD Systems", *China Commun.*, vol. 20, no. 6, pp. 100-115, June 2023.
[28] H. Xu, G. Zhou, K. -K. Wong, W. K. New, C. Wang, C. -B. Chae, R. Murch, S. Jin and Y. Zhang, "Channel Estimation for FAS-assisted Multiuser mmwave Systems", *IEEE Commun. Lett.*, vol. 28, no. 3, pp. 632-636, March 2024.
[29] F. Zhao, W. Chen, Z. Liu, J. Li and Q. Wu, "Deep Reinforcement Learning-based Intelligent Reflecting Surface Optimization for TDD Multi-user MIMO Systems", *IEEE Wirel. Commun. Lett.*, vol. 12, no. 11, pp. 1951-1955, Nov. 2023.
[30] D. Morejón, J. Montalbán, E. Iradier, M. Kashef Hany, R. Candell and P. Angueira, "Empirical Characterization of Doppler in Industrial Cireless channels", In Proceedings of the 18th European Conference on Antennas and Propagation (EuCAP), Glasgow, UK, 2024, pp. 1-5.
[31] L. Yao, L. Peng, G. Li, H. Fu and A. Hu, "A Simulation and Experimental Study of Channel Reciprocity in TDD and FDD Wiretap Channels", In Proceedings of the IEEE 19th International Conference on Communication Technology (ICCT), Xi'an, China, 2019, pp. 113-117.
[32] N. A. Moghaddam, A. Maleki and A. R. Sharafat, "Peak-to-average Power Ratio Reduction in LTE-advanced Systems Using Low Complexity and Low Delay PTS", *IET Commun.*, vol. 14, no. 11, pp. 1768-1772, 2020.
[33] G. Azarnia, A. A. Sharifi and H. Emami,"Compressive Sensing Based PAPR Reduction in OFDM Systems: Modified Orthogonal Matching Pursuit Approach", *ICT Express*, vol. 6, no. 4, pp. 368-371, 2020.
[34] S. Ramtej and S. Anuradha, "On Companding Techniques to Mitigate PAPR in SC-FDMA Systems", *Int. J. Wirel. Mob. Comput.*, vol. 18, no. 3, pp. 295-302, 2020.
[35] C. Xing, M. Xia, F. Gao and Y. -C. Wu, "Robust Transceiver with Tomlinson-Harashima Precoding for Amplify-and-Forward MIMO Relaying Systems", *IEEE J. Sel. Areas Commun.*, vol. 30, no. 8, pp. 1370-1382, Sept. 2012.
[36] Y. Li, M. Xia, and Y. -C. Wu, "Energy-Efficient Precoding for Non-Orthogonal Multicast and Unicast Transmission via First-Order Algorithm", *IEEE Trans. Wirel. Commun.*, vol. 18, no. 9, pp. 4590-4604, Sept. 2019.
[37] Y. A. Jawhar, K. Ramli, M. A. Taher, N. S. Shah, S. Mostafa and B. A. Khalaf, "Improving PAPR Performance of Filtered OFDM for 5G Communications Using PTS", *ETRI Journal Wiley*, vol. 43, no. 2, pp. 209-220, 2021.
[38] K. Zhong, Y. -C. Wu and S. Li, "Signal Detection for OFDM-Based Virtual MIMO Systems under Unknown Doubly Selective Channels, Multiple Interferences and Phase Noises", *IEEE Trans. Wirel. Commun.*, vol. 12, no. 10, pp. 5309-5321, Oct. 2013.
[39] A. M. Musa, R. Mokhtar, R. Saeed, H. Alhumyani, S. A. Khalek and A. Y. Mohamed, "Distributed SC-FDMA Sub-carrier Assignment for Digital Mobile Satellite", *Alexandria Eng. J.* vol. 60, no. 6, pp. 4973-4980, 2021.

[40] J. Chen, Y. -C. Wu, S. Ma and T. -S. Ng, "Joint CFO and Channel Estimation for Multiuser MIMO-OFDM Systems with Optimal Training Sequences", *IEEE Trans. Signal Process.*, vol. 56, no. 8, pp. 4008-4019, Aug. 2008.

[41] T. Li, Z. Tong, W. Zhang, Y. Liu and M. Wang, "Low-complexity PAPR Reduction Scheme Selective Mapping Cascading Improved μ Law Companding in CO-OFDM System", *Wirel. Pers. Commun.*, vol. 122, no. 1, pp. 861-876, 2022.

[42] H. Li, C. Huang, C. X. Wang and J. Li, "Scenario Classification and Channel Modeling for MIMO Communications in Dense Urban Street Scenarios", In Proceedings of the 18th European Conference on Antennas and Propagation (EuCAP), Glasgow, UK, 2024, pp. 1-5.

[43] J. Bao, Z. Cui, Y. Miao, Q. Zhu, B. Hua, K. Mao and H. Ni, "Impact of 6G Mobility on Doppler Characteristics of UAV-to-Vehicle Channels", In Proceedings of the 18th European Conference on Antennas and Propagation (EuCAP), Glasgow, UK, 2024, pp. 1-5, 2024.